

Figure 1. (a) SEM image and (b) HRTEM image of silicon quantum dots (Si-QDs).

450 nm absorption of formazans produced by the enzyme was measured with an E max (Molecular Devices, USA) microplate reader ($n = 2-6$). The activities were calculated as the ratio of the absorbance value against those of the control. For the measurement of LDH releases from cells, we used an LDH Cytotoxicity Detection Kit (Takara Bio, Japan) as an indicator for plasma membrane leakage ($n = 5$). The 490 nm absorption of formazans as an indicator of LDH releases were measured with the E max microplate reader. The cytotoxicity was calculated as the ratio of the LDH release from the sample against that of the positive control for cell-death, which was co-cultured with 200 μM CdCl₂ (Wako Pure Chemicals, Japan), and the negative control, which was cultured in MEM- α . For statistical analysis, the data were analysed using the Tukey–Kramer’s test for multi-group comparison. Differences were considered significant at $P < 0.05$.

2.5. Radical assays

Radical species was measured with a LumiMax Superoxide Anion Detection Kit (Stratagene, USA). Si-QDs in the concentration of 1120 $\mu\text{g ml}^{-1}$ were mixed with the reagents of the kit 10 min before the measurements. The chemiluminescence as an indicator of oxiradicals was measured with a microplate fluorometer, Fluoroskan Ascent FL (Thermo scientific, USA), with 5 min intervals ($n = 2$). Lipid peroxidation was assayed with a BioxTech MDA-586 assay kit (OXIS International, USA). The cells were cultured with Si-QDs at the concentration of 1120 $\mu\text{g ml}^{-1}$ for 48 h, the same as for the cytotoxicity assay ($n = 2$). As an indicator of

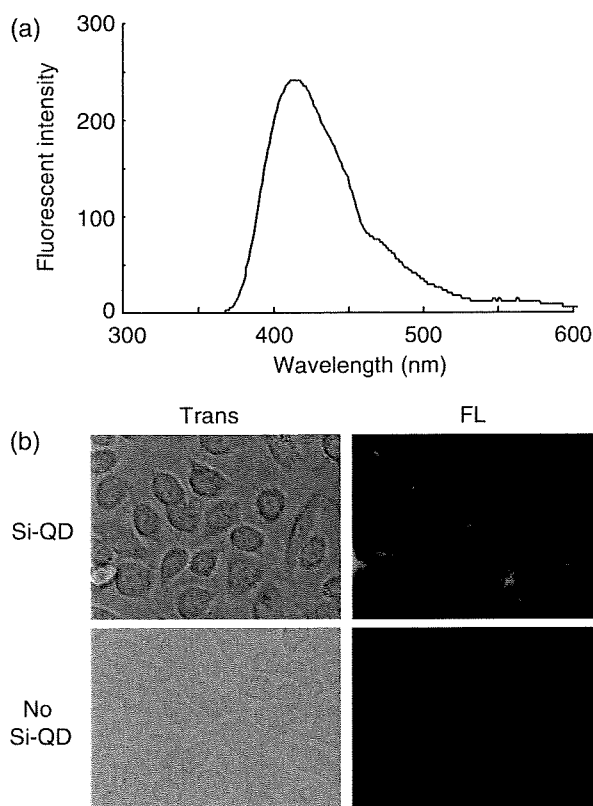


Figure 2. (a) Photoluminescent spectrum of Si-QDs excited at 300 nm. (b) Transmitted (trans) and fluorescent (FL) microscopy images of HeLa cells labelled with Si-QDs for 48 h incubation (upper), and without Si-QDs (lower).

(This figure is in colour only in the electronic version)

peroxy radicals, we assayed malondialdehyde, which can react with *N*-methyl-2-phenylindole and yield a stable chromophore with maximal absorbance at 586 nm, using an Ultrospec 2100 pro (GE Healthcare, UK) absorbance spectrometer.

3. Results and discussion

3.1. Characterization and bioimaging studies

Figure 1(a) shows the SEM image of a number of water-soluble Si-QDs on a carbon grid. The mean diameter of Si-QDs was 6.5 ± 1.5 nm. The TEM image shows the core structure of Si-QDs (figure 1(b)). The average structure size was 2.5 nm.

The photoluminescence spectrum in the phosphate buffered saline (PBS) excited at 300 nm shows a peak at 414 nm (figure 2(a)). The suitability of Si-QDs as a chromophore for biological imaging is demonstrated in figure 2(b). The Si-QDs were incubated with HeLa cells for 48 h and observed with a fluorescence microscope. Compared to the control, which was cultured in no-particle media, green fluorescence was observed brightly in the HeLa cells cultured with the Si-QDs. From this result, the green fluorescence has arisen from the emission of Si-QDs. Furthermore, the fluorescence was observed mainly on the cell surface.

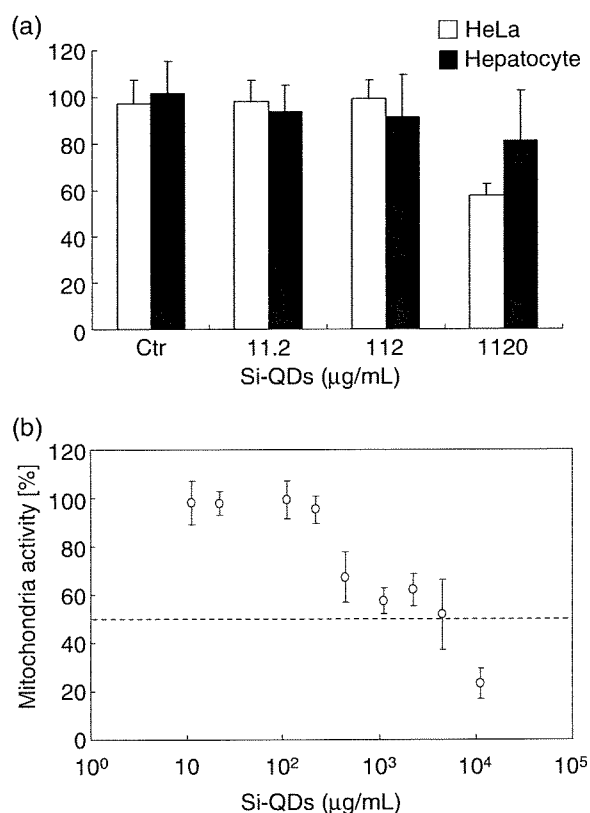


Figure 3. Effects of QDs on human cells. (a) Comparison of Si-QD toxicity against HeLa cells and hepatocytes. (b) Mitochondrial activity of HeLa cells cultured with Si-QDs.

These findings indicated the possibility of the Si-QDs as chromophores in bioimaging.

3.2. *In vitro* cytotoxicity and TC50

In order to use Si-QDs widely in bioimaging, we have to know the limit concentration at which the Si-QDs do not affect cell activity.

First, we measured the mitochondrial activities in 0–1120 $\mu\text{g ml}^{-1}$ of Si-QDs with HeLa cells as a carcinoma cell line, and also primary human hepatocytes for the simulation of *in vivo* toxicity. Mitochondrial activity assays indicate cell viability. As shown in figure 3(a), the Si-QDs at 1120 $\mu\text{g ml}^{-1}$ were less toxic against the hepatocytes than HeLa cells. Since our previous study also showed that HeLa cells were more sensitive to the toxicity test than hepatocytes [18], we used HeLa cells in further toxicity tests. In figure 3(b), we show the mitochondrial activities of HeLa cells in 11.2–11200 $\mu\text{g ml}^{-1}$ of Si-QDs. From the result, we calculated the 50%-inhibitory toxicity concentration (TC50) with HeLa cells as 4761 $\mu\text{g ml}^{-1}$.

Second, in comparison with CdSe-QDs, we performed two types of cytotoxicity assay: a mitochondrial activity assay, and a lactate dehydrogenase (LDH) release assay, which indicates cellular membrane damages. The cells were cultured with the QDs in the medium for 48 h and tested. Additionally,

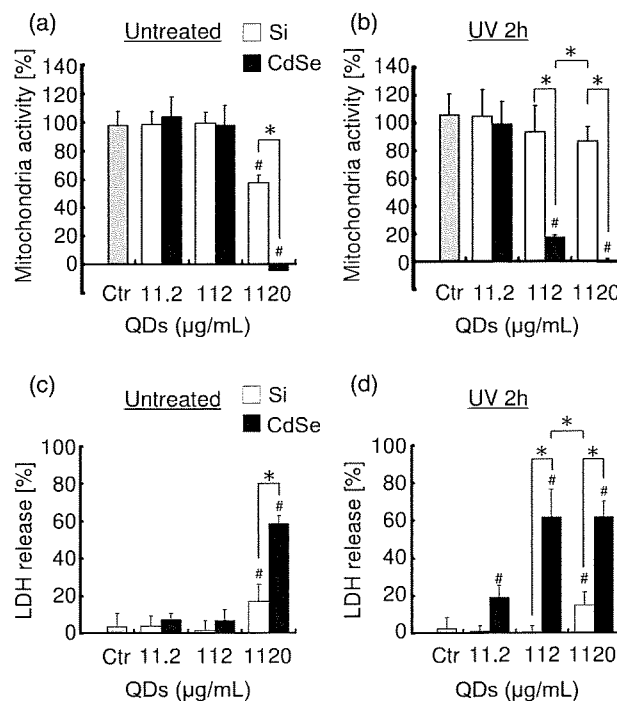


Figure 4. Comparison of QD toxicity on the mitochondrial activity ((a), (b)) and the LDH release ((c), (d)) after 48 h incubation. HeLa cells were incubated with untreated QDs ((a), (c)) and UV-exposed (2 h) QDs ((b), (d)). Si: Si-QDs, CdSe: CdSe-QDs. Values are mean \pm standard deviations. # represents the value being significantly different from the control ($P < 0.05$). * represents the difference being significant ($P < 0.05$).

in order to investigate the effects of degradation, we also used the QDs exposed to UV (254 nm) for 2 h before the co-culture.

Figure 4(a) shows the results of the mitochondrial activity assays with untreated Si-QDs. At a concentration of 1120 $\mu\text{g ml}^{-1}$, the mitochondrial activity with the Si-QDs decreased to $57 \pm 5.3\%$ of control ($P < 0.01$), which was significantly higher than that of CdSe-QDs ($P < 0.01$) (figure 4(a)). Additionally, with the UV-exposed Si-QDs at 1120 $\mu\text{g ml}^{-1}$, the activity decreased to $87 \pm 10\%$ (n.s.) and it was significantly higher than that of CdSe-QDs at 112 $\mu\text{g ml}^{-1}$ ($P < 0.01$) (figure 4(b)).

In the LDH assays, at a concentration of 1120 $\mu\text{g ml}^{-1}$, the LDH release with Si-QDs increased to $17 \pm 9.0\%$ ($P < 0.01$), which was significantly lower than that of CdSe-QDs ($P < 0.01$) (figure 4(c)). Using the UV-exposed Si-QDs at 1120 $\mu\text{g ml}^{-1}$, the release increased $15 \pm 6.8\%$ ($P < 0.05$) (figure 4(d)). In concentrations of more than 11.2 $\mu\text{g ml}^{-1}$, the releases with Si-QDs are significantly lower than those with CdSe-QDs at the same concentrations ($P < 0.01$) (figure 4(d)).

These results from both cytotoxicity assays suggested that we should use Si-QDs at concentrations less than 112 $\mu\text{g ml}^{-1}$. However, Si-QDs were less toxic than CdSe-QDs against the HeLa cells at 1120 $\mu\text{g ml}^{-1}$. In particular, after being exposed to UV, the Si-QDs were at least ten times less toxic than the CdSe-QDs in concentrations more than 112 $\mu\text{g ml}^{-1}$.

The cytotoxicities of several QDs have been reported [17, 19, 20, 42, 43]. Derfus *et al* studied the cytotoxicity of UV-exposed CdSe-QDs against hepatocytes and indicated that the cell damages were caused by cadmium ions released from CdSe-QDs [17]. We also identified that cadmium ions were released from our CdSe-QDs in similar conditions, such as UV or H₂O₂ exposure (UV exposure for 2 h: 48 ppm; H₂O₂ exposure for 48 h: 3.6 ppm). This result suggested that cadmium ions are released from CdSe-QDs in highly oxidative conditions and that they then degrade, and then the ions induce cytotoxicity.

On the other hand, the cytotoxicity of Si-QDs and its mechanism has not been reported. Compared to CdSe-QDs, Si-QDs do not consist of inherently toxic elements. There are some reports that several nanocrystals, such as fullerenes and CdTe-QDs, produced reactive oxygen species and that the radicals induced cell damage [19, 20, 43, 44]. Since Si-QDs at high concentration caused LDH release, an indicator of cellular membrane damage, we suspected that Si-QDs produced oxygen radicals and that the radicals affect the cell membrane.

3.3. Toxicity mechanism of silicon quantum dots

To test the hypothesis that cell toxicity caused by Si-QDs is due to radicals, we investigated the ability of Si-QDs to provide oxygen radicals and detected the peroxy radicals in co-cultured cells. In the presence of oxygen radical species, peroxy radicals are formed on the alkene termini of the cellular lipid bilayer and they can associate, forming a hole in cytoplasmic membrane [45].

First, we confirmed the ability of Si-QDs to provide oxygen radicals using a luminol reaction. Figure 5(a) shows that Si-QDs in aqueous solutions can produce oxygen radicals. The maximum yield of oxygen radicals from Si-QDs was seven times higher and their generations were longer in duration than those of the CdSe-QDs (figure 5(a)). When Si-QDs were exposed to UV, the maximum yield was lower than for untreated Si-QDs (figure 5(a)). These results suggested that Si-QDs produce oxygen radicals more readily than CdSe-QDs and that the yields are reduced by UV exposure.

Second, we confirmed the formation of peroxy radicals in the co-cultured cells with malondialdehyde (MDA) as the indicator of peroxy radicals. We show in figure 5(b) that the concentration of peroxy radicals increased with 1120 $\mu\text{g ml}^{-1}$ of Si-QDs with and without UV exposure. The mean concentration of the peroxy radicals in untreated Si-QDs was higher than that of UV-exposed Si-QDs.

Taken together, these radical results suggested that Si-QDs produce oxygen radicals and then the radicals affect the cytoplasmic membrane. Since the yields of oxygen radicals were reduced by UV exposure, the mechanism may be associated with the oxidative states of Si-QDs. Our previous study showed that the surface condition of Si-QDs was changed by oxidation [38, 39]. In addition, their surface potentials were reduced by UV exposure (data not shown).

Nanocrystals, such as fullerenes and CdTe-QDs, can also produce radical species, and the toxicities were reduced

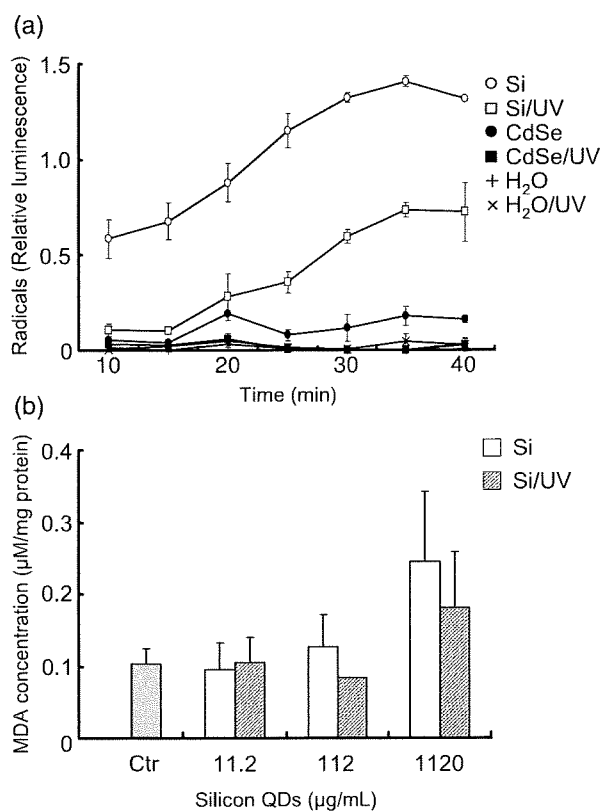


Figure 5. (a) Oxygen radical detection in QD solutions. QDs with and without UV exposure were incubated with luminol, and the chemiluminescence was measured at 5 min intervals after 10 min pre-incubation. Si: Si-QDs; Si/UV: UV-exposed Si-QDs; CdSe: CdSe-QDs; CdSe/UV: UV-exposed CdSe-QDs; H₂O: H₂O without UV exposure; H₂O/UV: H₂O with UV exposure. (b) Peroxy radical detection from the HeLa cells cultured with Si-QDs with and without UV exposure. Malondialdehyde (MDA) was used as the peroxy radical indicator. Si: Si-QDs. Si/UV: UV-exposed (2 h) Si-QDs. Values are mean \pm standard deviations.

by surface modification [20, 44]. Sayes *et al* showed that the cytotoxicity of fullerenes was changed by their surface functional group [44]. Choi *et al* showed that the modification with *N*-acetylcysteine (NAC), which has antioxidant property [46], reduced the lipid peroxidation from CdTe-QDs [20]. In this study, we showed the reduction of radicals with UV exposure (figure 5(a)). Although the Si-QDs showed less toxicity than the CdSe-QDs at high concentration, in order to be a much safer chromophore *in vivo* and to protect the environment, Si-QDs also need a suitable surface modification, such as NAC, and oxidative-state control with UV exposure. This study may therefore provide the basis for future improvements on the cytotoxicity amelioration of Si-QDs and safety precautions required.

4. Conclusion

In conclusion, passive-oxidized Si-QDs can be used as bioimaging probes. The mitochondrial activity assays and LDH release assays revealed that the Si-QDs were safer than CdSe-QDs at high concentration, especially under UV

exposure conditions. However, the Si-QDs may become slightly toxic to cultured human cells at high concentration. As one of the toxicity mechanisms, we suggest that oxygen radicals from Si-QDs affect the plasma membrane of cells. These results are useful information to future applications of Si-QDs in biological and medical areas.

Acknowledgments

This work was supported by the Ministry of Health, Labour and Welfare of Japan (H19-nano-012), and partially supported by the Cosmetology Research Foundation and the Research Institute for Science and Technology of Tokyo Denki University. We thank Mr Masateru Shibata (JEOL) for providing us with the SEM image, Mr Hisashi Masago (JASCO) for helpful advice about the fluorescent stability, Dr Yasuhiro Natori (IMCJ) for help with the measurement of chemiluminescence, and Mr Kazuyuki Ito (IMCJ) for useful discussion and revision of the manuscript.

References

- [1] Rosenthal S J, Tomlinson I, Adkins E M, Schroeter S, Adams S, Swafford L, McBride J, Wang Y, DeFelice L J and Blakely R D 2002 Targeting cell surface receptors with ligand-conjugated nanocrystals *J. Am. Chem. Soc.* **124** 4586–94
- [2] Dubertret B, Skourides P, Norris D J, Noireaux V, Brivanlou A H and Libchaber A 2002 *In vivo* imaging of quantum dots encapsulated in phospholipid micelles *Science* **298** 1759–62
- [3] Jaiswal J K, Mattoussi H, Mauro J M and Simon S M 2003 Long-term multiple color imaging of live cells using quantum dot bioconjugates *Nat. Biotechnol.* **21** 47–51
- [4] Xu H *et al* 2003 Multiplexed SNP genotyping using the QbeadTM system: a quantum dot-encoded microsphere-based assay *Nucleic Acids Res.* **31** e43
- [5] Wu X, Liu H, Liu J, Haley K N, Treadway J A, Larson J P, Ge N, Peale F and Bruchez M P 2003 Immunofluorescent labeling of cancer marker Her2 and other cellular targets with semiconductor quantum dots *Nat. Biotechnol.* **21** 41–6
- [6] Chan W C, Maxwell D J, Gao X, Bailey R E, Han M and Nie S 2002 Luminescent quantum dots for multiplexed biological detection and imaging *Curr. Opin. Biotechnol.* **13** 40–6
- [7] Zhu L, Ang S and Liu W T 2004 Quantum dots as a novel immunofluorescent detection system for *Cryptosporidium parvum* and *Giardia lamblia* *Appl. Environ. Microbiol.* **70** 597–8
- [8] Mattoussi H, Mauro J M, Goldman E R, Anderson G P, Sundar V C, Mikulec F V and Bawendi M G 2000 Self-assembly of CdSe–ZnS quantum dot bioconjugates using an engineered recombinant protein *J. Am. Chem. Soc.* **122** 12142–50
- [9] Manabe N, Hoshino A, Liang Y, Goto T, Kato N and Yamamoto K 2006 Quantum dots as a drug tracer *in vivo* *IEEE Trans. Nanobiosci.* **5** 263–7
- [10] Xiao Y, Gao X, Gannot G, Emmert-Buck M R, Srivastava S, Wagner P D, Amos M D and Barker P E 2008 Quantitation of HER2 and telomerase biomarkers in solid tumors with IgY antibodies and nanocrystal detection *Int. J. Cancer* **122** 2178–86
- [11] Ghazani A A, Lee J A, Klostranec J, Xiang Q, Dacosta R S, Wilson B C, Tsao M S and Chan W C 2006 High throughput quantification of protein expression of cancer antigens in tissue microarray using quantum dot nanocrystals *Nano Lett.* **6** 2881–6
- [12] Eastman P S *et al* 2006 Qdot nanobarcode for multiplexed gene expression analysis *Nano Lett.* **6** 1059–64
- [13] Liang R Q, Li W, Li Y, Tan C Y, Li J X, Jin Y X and Ruan K C 2005 An oligonucleotide microarray for microRNA expression analysis based on labeling RNA with quantum dot and nanogold probe *Nucleic Acids Res.* **33** e17
- [14] Lucas L J, Chesler J N and Yoon J Y 2007 Lab-on-a-chip immunoassay for multiple antibodies using microsphere light scattering and quantum dot emission *Biosens. Bioelectron.* **23** 675–81
- [15] Sun J, Zhu M Q, Fu K, Lewinski N and Drezek R A 2007 Lead sulfide near-infrared quantum dot bioconjugates for targeted molecular imaging *Int. J. Nanomed.* **2** 235–40
- [16] Kobayashi H, Hama Y, Koyama Y, Barrett T, Regino C A, Urano Y and Choyke P L 2007 Simultaneous multicolor imaging of five different lymphatic basins using quantum dots *Nano Lett.* **7** 1711–6
- [17] Derfus A M, Chan W C W and Bhatia S N 2004 Probing the cytotoxicity of semiconductor quantum dots *Nano Lett.* **4** 11–8
- [18] Shiohara A, Hoshino A K H, Suzuki K and Yamamoto K 2004 On the cyto-toxicity caused by quantum dots *Microbiol. Immunol.* **48** 669–75
- [19] Lovric J, Bazzi H S, Cuie Y, Fortin G R A, Winnik F M and Maysinger D 2005 Differences in subcellular distribution and toxicity of green and red emitting CdTe quantum dots *J. Mol. Med.* **83** 377–85
- [20] Choi A O, Cho S J, Desbarats J, Lovric J and Maysinger D 2007 Quantum dot-induced cell death involves F as upregulation and lipid peroxidation in human neuroblastoma cells *J. Nanobiotechnol.* **5** 1
- [21] Harper J and Sailor M J 1996 Detection of nitric oxide and nitrogen dioxide with photoluminescent porous silicon *Anal. Chem.* **68** 3713–7
- [22] Lin V S, Motesharei K, Dancil K S, Sailor J and Ghadiri M R 1997 A porous silicon-based optical interferometric biosensor *Science* **278** 840–3
- [23] Bruchez M J, Moronne M, Gin P, Weiss S and Alivisatos A P 1998 Semiconductor nanocrystals as fluorescent biological labels *Science* **281** 2013–6
- [24] Li Z F and Ruckenstein E 2004 Water-soluble poly(acrylic acid) grafted luminescent silicon nanoparticles and their use as fluorescent biological staining labels *Nano Lett.* **4** 1463–7
- [25] Warner J H, Hoshino A, Yamamoto K and Tilley R D 2005 Water-soluble photoluminescent silicon quantum dots *Angew. Chem. Int. Edn* **44** 2–6
- [26] Wilcoxon J P, Samara G A and Provencio P N 1999 Optical and electronic properties of Si nanoclusters synthesized in inverse micelles *Phys. Rev. B* **60** 2704–14
- [27] Holmes J D, Ziegler K J, Doty R C, Pell L E, Johnston K P and Korgel B A 2001 Highly luminescent silicon nanocrystals with discrete optical transitions *J. Am. Chem. Soc.* **123** 3743–8
- [28] Murray C B, Norris D J and Bawendi M G 1993 Synthesis and characterization of nearly monodisperse CdE (E = sulfur, selenium, tellurium) semiconductor nanocrystallites *J. Am. Chem. Soc.* **115** 8706–15
- [29] Zou J, Basdwin R K, Pettigrew K W and Kauzlarich S M 2004 Solution synthesis of ultrastable luminescent siloxane-coated silicon nanoparticles *Nano Lett.* **4** 1181–6
- [30] Germanenko I N, Li S and Samy El-shall M 2001 Decay dynamics and quenching of photoluminescence from silicon nanocrystals by aromatic nitro compounds *J. Phys. Chem. B* **105** 59–66
- [31] Li X, He Y, Talukdar S S and Swihart M T 2003 Process for preparing macroscopic quantities of brightly photoluminescent silicon nanoparticles with emission spanning the visible spectrum *Langmuir* **19** 8490–6

- [32] Littau K A, Szajowski P J, Muller A J, Kortan A R and Brus L E 1993 A luminescent silicon nanocrystals colloid via high-temperature aerosol reaction *J. Phys. Chem.* **97** 1224–30
- [33] English D S, Pell L E, Yu Z H, Barbara P F and Korgel B A 2002 Size tunable visible luminescence from individual organic monolayer stabilized silicon nanocrystal quantum dots *Nano Lett.* **2** 681
- [34] Takagi H, Ogawa H, Yamazaki Y, Ishizaki A and Nakagiri T 1990 Quantum size effects on photoluminescence in ultrafine Si particles *Appl. Phys. Lett.* **56** 2379–80
- [35] Wang J, Reipa V and Blasic J 2004 Silicon nanoparticles as a luminescent label to DNA *Bioconjug. Chem.* **15** 409–12
- [36] Hua F, Swihart M T and Ruckenstein E 2005 Efficient surface grafting of luminescent silicon quantum dots by photoinitiated hydrosilylation *Langmuir* **21** 6054–62
- [37] Hua F, Erogbogbo F, Swihart M T and Ruckenstein E 2006 Organically capped silicon nanoparticles with blue photoluminescence prepared by hydrosilylation followed by oxidation *Langmuir* **22** 4363–70
- [38] Shinoda K, Yanagisawa S, Sato K and Hirakuri K 2006 Stability of nanocrystalline silicon particles in solution *J. Cryst. Growth.* **288** 84–6
- [39] Hiruoka M, Sato K and Hirakuri K 2007 Correlation between surface composition and luminescence of nanocrystalline silicon particles dispersed in pure water *J. Appl. Phys.* **102** 024308
- [40] Ishiyama M, Miyazono Y, Sasamoto K, Ohkura Y and Ueno K 1997 A highly water-soluble disulfonated tetrazolium salt as a chromogenic indicator for NADH as well as cell viability *Talanta* **44** 1299–305
- [41] Tominaga H, Ishiyama M, Ohseto F, Sasamoto K, Hamamoto T, Suzuki K and Watanabe M 1999 A water-soluble tetrazolium salt useful for colorimetric viability assay *Anal. Commun.* **36** 47–50
- [42] Hoshino A, Fujioka K, Oku T, Suga M, Sasaki Y, Ohta T, Yasuhara M, Suzuki K and Yamamoto K 2004 Physicochemical properties and cellular toxicity of nanocrystals quantum dots depend on their surface modification *Nano Lett.* **4** 2163–9
- [43] Lovric J, Cho S J, Winnik F M and Maysinger D 2005 Unmodified cadmium telluride quantum dots induce reactive oxygen species formation leading to multiple organelle damage and cell death *Chem. Biol.* **12** 1227–34
- [44] Sayes C M *et al* 2004 The differential cytotoxicity of water-soluble fullerenes *Nano Lett.* **4** 1881–7
- [45] Buettner G 1993 The pecking order of free radicals and antioxidants: lipid peroxidation, alpha-tocopherol, and ascorbate *Arch. Biochem. Biophys.* **300** 535–43
- [46] Cotgreave I A 1997 *N*-acetylcystein: pharmacological considerations and experimental and clinical applications *Adv. Pharmacol.* **38** 205–27

